International Journal of Pharmaceutics 363 (2008) 73–77

Contents lists available at ScienceDirect

International Journal of Pharmaceutics

journal homepage: www.elsevier.com/locate/ijpharm

Theoretical comparison of hydrodynamic diffusion layer models used for dissolution simulation in drug discovery and development

Kiyohiko Sugano*

Global Research & Development, Research Formulation, Sandwich Laboratories, Pfizer, Inc., Ramsgate Road, CT13 9NJ Sandwich, Kent, UK

ARTICLE INFO

Article history:
Received 7 May 2008
Received in revised form 3 July 2008
Accepted 5 July 2008
Available online 15 July 2008

Keywords:
Dissolution
Hydrodynamic
Diffusion
Solubility
Particle
Simulation
Fluid dynamics

ABSTRACT

The effective hydrodynamic diffusion layer thickness (h_{eff}) of a drug particle dissolving into an agitated fluid is of great importance for oral absorption simulation. The purpose of the present study was to: (1) introduce a h_{eff} estimation method based on the fluid dynamic theory (FD model), and (2) compare the FD model with the non-FD-based approximation models previously reported by Hintz and Johnson (HJ model) and Wang and Flanagan (WF model). In the FD model, the relative velocity of a particle suspended in an agitated fluid was estimated from the terminal slip velocity and the microeddy effect. For small particles (particle radius (r_p) < ca. 15 μm), the HJ, WF and FD models resulted in the similar h_{eff} values, whereas they resulted in different h_{eff} values for large particles (r_p > ca. 15 μm). One of the merits of the FD model is that it provides the *a priori* theoretical estimation of h_{eff} from particle radius, drug density, agitation strength, fluid viscosity, and diffusion coefficient. The hydrodynamic conditions in the gastrointestinal (GI) tract differ among human and animals, the GI sites, and fasted/fed conditions, etc. Therefore, the FD model could provide a more comprehensive and sophisticated simulation of oral absorption.

1. Introduction

Computational simulation of oral absorption is one of the necessary tools in drug discovery and development (Kuentz et al., 2006; Parrott and Lave, 2002; Sugano et al., 2007; Wei and Loebenberg, 2006). Several oral absorption simulators are commercially available. Usually, an oral absorption simulator consists of many mathematical equations corresponding to each process of oral absorption, e.g., dissolution of a drug, intestinal membrane permeation, etc. (Yu and Amidon, 1999). One of the most important processes in oral absorption is the dissolution process.

In the pharmaceutical sciences, the dissolution process of a solid drug is mainly described by the Noyes–Whitney equation (Eq. (1)), and further by the Nernst–Brunner equation (NBE) (Eq. (2)) (Dokoumetzidis and Macheras, 2006; Noyes and Whitney, 1897). The NBE postulates the existence of an unstirred fluid layer (hydrodynamic diffusion layer (HDL)) on the solid surface:

$$\frac{dX}{dt} = k_{diss}(C_s - C_t) = SA\,k_{mass}(C_s - C_t) \quad (1)$$

$$\frac{dX}{dt} = SA\,D_{eff}\frac{1}{h_{eff}}(C_s - C_t) \quad (2)$$

where k_{diss} is the dissolution rate coefficient, k_{mass} is the mass transfer coefficient, SA is the solid surface area, D_{eff} is the effective diffusion coefficient, h_{eff} is the effective thickness of HDL, C_s is the solubility at the solid surface, and C_t is the concentration of the drug in the bulk fluid at time t. The purpose of the present study was to: (1) introduce an h_{eff} estimation method based on the fluid dynamic theory (FD model), and (2) compare the FD model with the non-FD based approximation models previously reported by Hintz and Johnson (HJ model) (Hintz and Johnson, 1989; Johnson, 2003; Lu et al., 1993), and Wang and Flanagan (WF model) (Wang and Flanagan, 1999, 2002).

2. Theory

2.1. Fluid dynamics model (FD model)

2.1.1. Dissolution rate equation in FD theory

The theory of mass transfer from/into suspended particles in an agitated fluid had been extensively investigated by fluid dynamics (Armenante and Kirwan, 1989; Chuchottaworn and Asano, 1986; Chuchottaworn et al., 1984; Harriott, 1962; Levins and Glastonbury, 1972a,b; Ranz and Marshall, 1952). According to the fluid dynamics theory, the mass transfer coefficient for a particle is described as:

$$k_{mass} = \frac{D_{eff}\,Sh}{L} = \frac{D_{eff}\,Sh}{d_p} \quad (3)$$

* Tel.: +44 1304 644338.
E-mail address: Kiyohiko.Sugano@pfizer.com.

0378-5173/$ – see front matter © 2008 Elsevier B.V. All rights reserved.
doi:10.1016/j.ijpharm.2008.07.002

Nomenclature

C_D	resistance coefficient from the fluid
C_s	solubility at solid surface
C_t	concentration of drug in bulk fluid at time t
d_p	particle diameter
D_{eff}	effective diffusion coefficient
D_{paddle}	diameter of paddle
g	gravity constant
$h_{c,HJ}$	boundary value for Hintz-Johnson model
$h_{c,WF}$	boundary value for Wang-Flanagan model
h_{eff}	effective thickness of hydrodynamic diffusion layer
k_{diss}	dissolution rate coefficient
k_{mass}	mass transfer coefficient
L	representative length of particle
N_{paddle}	rotation speed (rpm)
PN	power number specific for paddle shape
Re_p	Reynolds number of particle
SA	solid surface area
Sc	Schmidt number
Sh	Sherwood number
t	time
V_i	inertia slip velocity
V_{me}	relative effective velocity between particles and microeddies
$V_{rel,tot}$	total relative velocity of particle against fluid flow
V_t	terminal (sedimentation) slip velocity
Vol_{fluid}	volume of fluid

Greek symbols

ε	power input per unit mass
μ	viscosity of fluid
ν	kinematic viscosity of fluid
ρ_f	density of fluid
ρ_p	density of particle

where Sh is a dimensionless parameter, the Sherwood number, which represents the fluid dynamical characteristics of mass transfer by molecular diffusion and fluid flow. L is the representative length of the particle. For a spherical particle, L is the particle diameter (d_p). Comparing the Eqs. (2) and (3), h_{eff} is:

$$\frac{1}{h_{eff}} = \frac{Sh}{d_p} = \frac{Sh}{2r_p} \tag{4}$$

where r_p is the particle radius.

2.1.2. Sherwood number calculation

The Sherwood number can be related to the Reynolds number of the particle (Re_p) and the Schmidt number (Sc):

$$Sh = f(Re_p, Sc) \tag{5}$$

$$Re_p = \frac{d_p V_{rel,tot}}{\nu} \tag{6}$$

$$Sc = \frac{\nu}{D_{eff}} \tag{7}$$

where ν is the kinematic viscosity, and $V_{rel,tot}$ is the total relative velocity of the particle against the fluid flow. As a semi-empirical approximation, the Ranz–Marshall correlation is often used for a spherical particle (Ranz and Marshall, 1952):

$$Sh = 2 + 0.6\,Re_p^{1/2}\,Sc^{1/3} \tag{8}$$

The first term of Eq. (8) is derived as follows. As the distance away from the particle increases, the spherical surface area expands to produce a concentration gradient around the particle. Therefore, even without any flow ($V_{rel,tot} = 0$ and $Re_p = 0$. the *real* HDL thickness is infinite), a particle fixed in the fluid space dissolves into the fluid. This effect is called "asymptotic molecular diffusion" or "the curvature effect". It is well known, both theoretically and experimentally, that Sh from asymptotic molecular diffusion is 2 for a spherical particle. Therefore, maximum *effective* HDL thickness (h_{eff}) of a spherical particle is r_p (Eq. (4)).

The second term of Eq. (8) represents the effect of flow around a spherical particle. When the particle is suspended in the fluid, $V_{rel,tot}$ is not equal to the absolute flow speed because the particles move together with the fluid flow. Since ν, d_p, and D_{eff} can be easily obtained by an experiment or a calculation, once $V_{rel,tot}$ for a suspended particle in a flow is obtained, Re_p, Sh and h_{eff} can be calculated by Eqs. (6), (8) and (4), respectively.

2.1.3. Total relative velocity

$V_{rel,tot}$ mainly consists of: (1) the terminal (sedimentation) slip velocity (V_t), (2) the relative effective velocity between particles and microeddies (V_{me}), and (3) inertia slip velocity (V_i) (Levins and Glastonbury, 1972a,b):

$$V_{rel,tot} = \sqrt{V_t^2 + V_{me}^2 + V_i^2} \tag{9}$$

The contribution of V_i is small and neglected in this study (Levins and Glastonbury, 1972a,b).

2.1.3.1. Terminal slip velocity. The V_t of a spherical particle can be calculated as:

$$V_t = \left(\frac{4(\rho_p - \rho_f)d_p\,g}{3\rho_f}\,\frac{1}{C_D}\right)^{1/2} \tag{10}$$

where ρ_p is the density of a particle, ρ_f is the density of a fluid, g is the gravity constant, and C_D is the resistance coefficient from the fluid.

When $Re_p < 0.3$, C_D of a spherical particle can be derived from the Navier–Stokes equation with Stokes approximation as (Flemmer and Banks, 1986):

$$C_D = \frac{24}{Re_p} \tag{11}$$

$$V_t = \frac{(\rho_p - \rho_f)d_p^2 g}{18\mu} \tag{12}$$

where μ is the viscosity of the fluid. When $Re_p > 0.3$, C_D can be approximated by (Camenen, 2007):

$$C_D = \left[\left(\frac{A}{Re_p}\right)^{1/m} + B^{1/m}\right]^m \tag{13}$$

$$V_t = \frac{\nu}{d_p}\left(\sqrt{\frac{1}{4}\left(\frac{A}{B}\right)^{2/m} + \left(\frac{4}{3}\frac{d_{p*}^3}{B}\right)^{1/m}} - \frac{1}{2}\left(\frac{A}{B}\right)^{1/m}\right)^m \tag{14}$$

$$d_{p*} = \left(\left(\frac{\rho_p}{\rho_f} - 1\right) g \left(\frac{1}{\nu}\right)^2\right)^{1/3} d_p \tag{15}$$

Various A, B and m values have been reported depending on the Re_p range and particle shape. In this study, $A = 20.5$, $B = 0.310$ and $m = 2.07$ were used for spherical particles. These coefficients are obtained by fitting Eq. (13) to the experimental C_D values in $0.3 < Re_p < 100$ range (Kelbaliyev and Ceylan, 2007). The error was with in 1.1% (data not shown).

2.1.3.2. Developing boundary layer by microeddies. The V_{me} can be calculated based on the isotropic turbulence theory. If the density difference between the particle and fluid is zero, the terminal slip velocity and the inertia velocity become zero. Even in this case, however, the dissolution rate increases as the agitation strength increases because of the continuous formation and disappearance of microeddies that is the basis of the turbulent energy cascade process. Based on the Kolmogorov's hypothesis of local isotropy, Armentante and Kirwan suggested that the V_{me} can be expressed as (Armenante and Kirwan, 1989):

$$V_{me} = 0.195\, d_p^{1.1}\, \varepsilon^{0.525}\, \mu^{-0.575} \tag{16}$$

where ε is the power input per unit mass. No special case of V_{me} is made that represents a physical velocity. It is an expedient velocity which gives the same mass transfer. In the case of USP paddle methods, ε can be calculated as (Crail et al., 2004):

$$\varepsilon = \mathrm{PN}\, \rho_f\, N_{paddle}^3\, \frac{D_{paddle}^5}{\mathrm{Vol}_{fluid}} \tag{17}$$

where D_{paddle} is the diameter of the paddle, N_{paddle} is the rotation speed (rpm), and Vol_{fluid} is the volume of the fluid. PN is the power number specific for the shape of the paddle. With 50 rpm and 1 L fluid, $\varepsilon = 0.004\ \mathrm{m^2/s^3}$ (Crail et al., 2004). It is difficult to directly estimate ε value for in vivo gastrointestinal (GI) tract. It was reported that the agitation strength in the human GI tract corresponds to 20–75 rpm (Katori et al., 1995; Scholz et al., 2003). Therefore, ε value would be 0.0003–0.014 $\mathrm{m^2/s^3}$ range.

2.2. Hintz and Johnson model (HJ model)

Hintz and Johnson proposed a convenient approximation model of h_{eff} (Hintz and Johnson, 1989; Johnson, 2003; Lu et al., 1993):

$$h_{eff} = r_p, \quad r_p < h_{c,HJ} \tag{18}$$

$$h_{eff} = h_{c,HJ}, \quad r_p > h_{c,HJ} \tag{19}$$

where $h_{c,HJ}$ is the boundary value. Firstly, $h_{c,HJ} = 30\ \mu\mathrm{m}$ was derived based on rotate disk method. Later, the $h_{c,HJ}$ was estimated to be 18–30 μm from experimental dissolution data obtained by the UPS paddle method using particles of d_{50} < ca. 50 μm (900 mL, 75 rpm). In the present study, $h_{c,HJ}$ was set to 30 μm.

2.3. Wang and Flanagan model (WF model)

Recently, Wang and Flanagan proposed another model (Eq. (20)) based on the film theory considering the curvature of a spherical particle (Wang and Flanagan, 1999, 2002). In their theory, it was hypothesized that the real HDL thickness ($h_{c,WF}$) does not depend on the particle size (this hypothesis seems inconsistent with the fluid dynamic theory (Prandtl's boundary layer)).

$$\frac{1}{h_{eff}} = \frac{1}{r_p} + \frac{1}{h_{c,WF}} \tag{20}$$

The $h_{c,WF}$ was estimated to be 110 μm by fitting the equation to the experimental dissolution data obtained by the flow through experiment (particles were fixed on a filter). In addition, $h_{c,WF}$ was estimated to be 69.5–322 μm for the suspended particles under strong agitation conditions (500 rpm) (both experiments used d_p = 100–1000 μm particles). In the present study, $h_{c,WF}$ was set to 110 μm. If $r_p \ll h_{c,WF}$, $h_{eff} = r_p$ and if $r_p \gg h_{c,WF}$, $h_{eff} = h_{c,WF}$. Therefore, at small and large h_{eff} range, when we set $h_{c,HJ} = h_{c,WF}$, the WF model equals to the HJ model.

3. Results and discussion

The mass transfer phenomena have been intensively investigated in fluid dynamics (Armenante and Kirwan, 1989; Chuchottaworn and Asano, 1986; Chuchottaworn et al., 1984; Harriott, 1962; Levins and Glastonbury, 1972a,b; Ranz and Marshall, 1952). The effects of agitation strength, fluid viscosity, fluid density, particle density, particle shape, etc., on the mass transfer coefficient are described in terms of dimensionless parameters, such as Sherwood number, Reynolds number and Schmitt number. The fluid dynamic theory provides the means for *a priori* calculation of Sh (therefore, h_{eff}) from these parameters. Since the fluid dynamic theory of mass transfer had been sufficiently validated for a wide range of experimental conditions, a further experimental validation study was not performed in the present study (Armenante and Kirwan, 1989; Levins and Glastonbury, 1972b). On the other hand, the HJ model and WF model is not based on the fluid dynamic theory, and $h_{c,HJ}$ and $h_{c,WF}$ were obtained by fitting to experimental data of a specific experimental condition and particle size. Therefore, it would be of great interest to compare these models with the FD model.

The relationship between h_{eff} and r_p for a drug of $D_{eff} = 6.5 \times 10^{-6}\ \mathrm{cm^2/s}$ in water at 37 °C ($\nu = 0.70 \times 10^{-6}\ \mathrm{m^2/s}$, $\rho_f = 1.0\ \mathrm{g/cm^3}$) is summarized in Table 1, and plotted in Figs. 1 and 2. In addition, the initial dissolution rate (DR_{ini}) is plotted against r_p (drug amount = 1 mg, $C_s = 0.1$ mg/mL, $\rho_p = 1.2\ \mathrm{g/cm^3}$, monodispersed particle) (Figs. 1 and 2, and summarized in Table 2). DR_{ini} was calculated as previously reported (Hintz and Johnson, 1989). The density of the drug (ρ_p) was changed from 1.0 to

Table 1
h_{eff} calculated by the FD model[a]

r_p (μm)	h_{eff} (μm)										
	ρ_p (g/cm³)[b]						ε (m²/s³)[c]				
	1	1.05	1.1	1.2	1.4	1.8	0.0005	0.004	0.013	0.032	0.26
0.5	0.49	0.49	0.49	0.49	0.49	0.49	0.5	0.49	0.49	0.49	0.48
1	0.98	0.98	0.98	0.98	0.98	0.98	0.99	0.98	0.97	0.96	0.94
2.5	2.4	2.4	2.4	2.4	2.4	2.4	2.4	2.4	2.3	2.3	2.1
5	4.4	4.4	4.4	4.4	4.4	4.4	4.6	4.4	4.3	4.1	3.6
10	7.9	7.9	7.9	7.9	7.8	7.6	8.6	7.9	7.3	6.9	5.6
25	15	15	15	14	14	12	16	14	13	11	8.2
50	21	21	20	18	16	13	20	18	16	14	9.6
100	25	24	23	20	16	13	21	20	18	16	10
250	29	26	23	19	15	12	20	19	18	16	10
500	30	26	23	19	15	13	20	19	17	16	10

[a] $\nu = 0.70 \times 10^{-6}\ \mathrm{m^2/s}$, $\rho_f = 1.0\ \mathrm{g/cm^3}$.
[b] $\varepsilon = 0.004\ \mathrm{m^2/s^3}$.
[c] $\rho_p = 1.2\ \mathrm{g/cm^3}$.

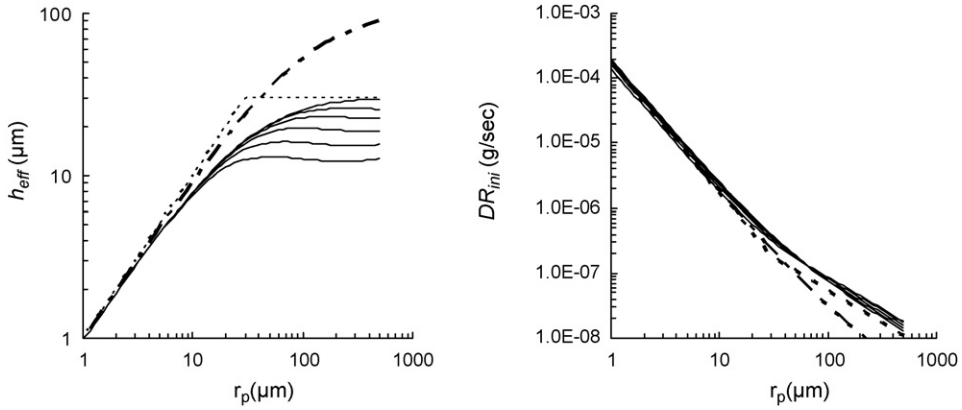

Fig. 1. Effect of drug density on the relationship between r_p and h_{eff} (A) or DR_{ini} (B). The order of the solid line at r_p = 500 μm is 1, 1.05, 1.1, 1.2, 1.4 and 1.8 g/cm^3 from the top for h_{eff} and from the bottom for DR_{ini}. The dotted line is the HJ model ($h_{c,HJ}$ = 30 μm). The dot–dash line is WF model ($h_{c,WF}$ = 110 μm). ε = 0.004 m^2/s^3 (equivalent to 50 rpm in 1 L USP paddle method). D_{eff} = 6.5 × 10^{-6} cm^2/s. ν = 0.7 × 10^{-6} m^2/s. ρ_f = 1.0 g/cm^3. The drug amount and solubility for DR_{ini} calculation were 1 mg and C_s = 100 μg/mL, respectively.

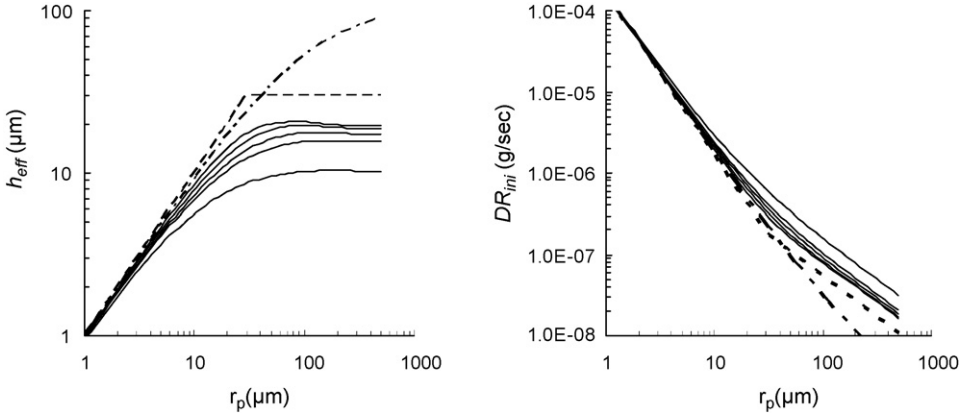

Fig. 2. Effect of agitation strength on the relationship between r_p and h_{eff} (A) or DR_{ini} (B). The solid line order at 500 μm is 0.0005, 0.004, 0.013, 0.032 and 0.26 m^2/s^3 from the top for h_{eff} and from the bottom for DR_{ini}. The dotted line is the HJ model ($h_{c,HJ}$ = 30 μm). The dot–dash line is WF model ($h_{c,WF}$ = 110 μm). ρ_p = 1.2 g/cm^3. D_{eff} = 6.5 × 10^{-6} cm^2/s. ν = 0.7 × 10^{-6} m^2/s. ρ_f = 1.0 g/cm^3. The drug amount and solubility for DR_{ini} calculation were 1 mg and C_s = 100 μg/mL, respectively.

1.8 g/cm^3, and the power input per unit mass (ε) was changed from 0.0005 to 0.26 m^2/s^3 which is equivalent to 25–200 rpm in 1 L USP paddle method. In the FD model, for most cases, Re_p was < 100 ($Re_p \approx 100$ for r_p = 300 μm, ρ_p = 1.8 g/cm^3 and ε = 0.26 m^2/s^3).

For small particles (r_p < ca. 15 μm), the V_t and V_{me} is negligible and the mass transfer is dominated by the asymptotic molecular diffusion (Sh = 2, $h_{eff} = r_p$). All models converge to the asymptotic molecular diffusion line (Figs. 1 and 2). Particle density and agitation strength have little effect on h_{eff}. It is experimentally well known that the agitation strength has little effect on the mass transfer for small particles (down to nano-scale) (Galli, 2006), whereas it does affect the mass transfer for large particles. However, parti-

Table 2
DR_{ini} calculated by the FD model[a]

r_p (μm)	DR_{ini} (mg/s)[b]										
	ρ_p (g/cm^3)[c]						ε (m^2/s^3)[d]				
	1	1.05	1.1	1.2	1.4	1.8	0.0005	0.0040	0.013	0.032	0.26
0.5	0.79	0.75	0.72	0.66	0.56	0.44	0.65	0.66	0.66	0.66	0.67
1	0.2	0.19	0.18	0.17	0.14	0.11	0.16	0.17	0.17	0.17	0.17
2.5	0.033	0.032	0.03	0.028	0.024	0.018	0.027	0.028	0.028	0.029	0.031
5	0.0088	0.0084	0.008	0.0073	0.0063	0.0049	0.007	0.0073	0.0076	0.0079	0.0089
10	0.0025	0.0023	0.0022	0.0021	0.0018	0.0014	0.0019	0.0021	0.0022	0.0024	0.0029
25	0.00053	0.0005	0.00048	0.00045	0.00041	0.00036	0.0004	0.00045	0.00051	0.00057	0.00079
50	0.00019	0.00018	0.00018	0.00018	0.00018	0.00017	0.00016	0.00018	0.0002	0.00023	0.00034
100	0.000077	0.000076	0.000078	0.000083	0.000087	0.000086	0.000079	0.000083	0.000092	0.0001	0.00016
250	0.000027	0.000029	0.000031	0.000034	0.000036	0.000035	0.000033	0.000034	0.000037	0.000041	0.000063
500	0.000013	0.000014	0.000016	0.000017	0.000018	0.000017	0.000017	0.000017	0.000019	0.000021	0.000032

[a] Drug amount = 1 mg, ν = 0.70 × 10^{-6} m^2/s, ρ_f = 1.0 g/cm^3.
[b] Cs = 0.1 mg/mL, D_{eff} = 6.5 × 10^{-6} cm/s.
[c] ε = 0.004 m^2/s^3.
[d] ρ_p = 1.2 g/cm^3.

cle density affects DR_{ini} since it changes the surface area per drug weight (Table 2). For large particles (r_p > ca. 15 μm), the results from the HJ, WF and FD models differed. In the FD model, as r_p increases, V_t, V_{me} and Re_p increase, resulting in an increase of Sh. However, h_{eff} stays at an almost constant value with r_p > ca. 50 μm, since the increase in Sh is cancelled out by r_p in the denominator (Eq. (4), Figs. 1 and 2). The shape and plateau value of the $h_{eff} - r_p$ curve depends on particle density and agitation strength.

When $h_{c,HJ}$ = 30 μm and $h_{c,WF}$ = 110 μm were employed, both the HJ model and WF model predict slower dissolution rates compared to the FD model. To approximate the FD model by the HJ and WF model, the $h_{c,HJ}$ and $h_{c,WF}$ can be changed. In the HJ model, $h_{c,HJ}$ = ca. 20 μm would be more appropriate for the particles of ρ_p = 1.05–1.4 g/cm^3 under ε = 0.0005–0.032 m^2/s^3 (25–100 rpm in USP paddle method). In the WF model, $h_{c,WF}$ = ca. 30 μm would give a similar result to the FD model (r_p < ca. 75 μm range). It should be remembered that these approximations are valid for suspended particles but invalid for particles under other flow conditions.

It is interesting that, according to the FD model, the drug density has little effect on DR_{ini} around $r_p \approx 70$ μm (Fig. 2). As the drug density increases, the terminal slip velocity of the particle increases (hence $h_{eff} \downarrow$ and $k_{mass} \uparrow$), and simultaneously, the surface area per unit weight of the drug decreases (if the particle radius is same, as the density increases, the weight of one particle increases, the number of the particles per unit drug weight decreases, and the total surface area of unit drug weight decreases).

One of the merits of the FD model is that it provides the theoretical *a priori* estimation of h_{eff} (Figs. 1 and 2 and Table 1). It enables the estimation of h_{eff} for wide range of agitation strengths, drug densities, fluid viscosity, etc. The agitation strength and the viscosity of GI fluid differ depending on species, the GI site, and fasted/fed condition, etc. (Kamba et al., 2002). The FD model provides the basis for the more sophisticated simulation of oral absorption. To simulate the dissolution in the gastrointestinal tract, the effective diffusion coefficient and viscosity which are relevant to the intestinal fluid should be used (Okazaki et al., 2008). The equation for terminal slip velocity used in this study is a complete solution. It does not require an iterative calculation (many V_t approximate equations require iterative calculations). Therefore, little calculation expense is required for numerical simulation.

The present study focused on the spherical particles. For non-spherical particles, the terminal slip velocity equation (Eqs. (10) and (13)) and the Ranz–Marshall equation (Eq. (8)) can be further modified (Camenen, 2007; Chuchottaworn and Asano, 1986).

Sedimentation of the particles might occur as the drug density increases, the particle size increases, and/or the agitation strength decreases. In such cases, $V_{rel,tot}$ cannot be appropriately calculated by Eqs. (10)–(17). The dissolution from the sediment (on the intestinal wall, the vessel bottom, etc.) would be smaller than that predicted by the models in this study. Information about the minimum agitation strength for complete suspension would be helpful.

Further detailed and more accurate calculation of mass transfer from suspended particles would require computational fluid dynamic (CFD) calculation (numerical integration of the Navier–Stokes equation) (Bai et al., 2007; McCarthy Leonard et al., 2004; Misumi et al., 2004). At present, the CFD calculation would be difficult to apply to oral absorption simulations considering the practical usage in drug discovery and development.

In conclusion, the HJ, WF and FD models, resulted in the similar h_{eff} in smaller particle size range, whereas they resulted in different h_{eff} in larger particle size range. The FD model provides the basis for the more sophisticated dissolution simulation of suspended drug particle. The FD model would be applicable for various fluid conditions of *in vivo* GI tracts and *in vitro* dissolution test apparatus.

References

Armenante, P.M., Kirwan, D.J., 1989. Mass transfer to microparticles in agitated systems. Chem. Eng. Sci. 44, 2781–2796.

Bai, G., Armenante, P.M., Plank, R.V., Gentzler, M., Ford, K., Harmon, P., 2007. Hydrodynamic investigation of USP dissolution test apparatus II. J. Pharm. Sci. 96, 2327–2349.

Camenen, B., 2007. Simple and general formula for the settling velocity of particles. J. Hydraul. Eng. 133, 229–233.

Chuchottaworn, P., Asano, K., 1986. Numerical analysis of drag coefficients and the heat and mass transfer of spheroidal drops. J. Chem. Eng. Jpn. 19, 208–213.

Chuchottaworn, P., Fujinami, A., Asano, K., 1984. Numerical analysis of heat and mass transfer from a sphere with surface mass injection or suction. J. Chem. Eng. Jpn. 17, 1–7.

Crail, D.J., Tunis, A., Dansereau, R., 2004. Is the use of a 200 ml vessel suitable for dissolution of low dose drug products? Int. J. Pharm. 269, 203–209.

Dokoumetzidis, A., Macheras, P., 2006. A century of dissolution research: from Noyes and Whitney to the biopharmaceutics classification system. Int. J. Pharm. 321, 1–11.

Flemmer, R.L.C., Banks, C.L., 1986. On the drag coefficient of a sphere. Powder Technol. 48, 217–221.

Galli, C., 2006. Experimental determination of the diffusion boundary layer width of micron and submicron particles. Int. J. Pharm. 313, 114–122.

Harriott, P., 1962. Mass transfer to particles. Part 1. Suspended inagitated tanks. AIChE J. 8, 93–102.

Hintz, R.J., Johnson, K.C., 1989. The effect of particle size distribution on dissolution rate and oral absorption. Int. J. Pharm. 51, 9–17.

Johnson, K.C., 2003. Dissolution and absorption modeling: model expansion to simulate the effects of precipitation, water absorption, longitudinally changing intestinal permeability, and controlled release on drug absorption. Drug Dev. Ind. Pharm. 29, 833–842.

Kamba, M., Seta, Y., Kusai, A., Nishimura, K., 2002. Comparison of the mechanical destructive force in the small intestine of dog and human. Int. J. Pharm. 237, 139–149.

Katori, N., Aoyagi, N., Terao, T., 1995. Estimation of agitation intensity in the GI tract in humans and dogs based on in vitro/in vivo correlation. Pharm. Res. 12, 237–243.

Kelbaliyev, G., Ceylan, K., 2007. Development of new empirical equations for estimation of drag coefficient, shape deformation, and rising velocity of gas bubbles or liquid drops. Chem. Eng. Commun. 194, 1623–1637.

Kuentz, M., Nick, S., Parrott, N., Rothlisberger, D., 2006. A strategy for preclinical formulation development using GastroPlus(TM) as pharmacokinetic simulation tool and a statistical screening design applied to a dog study. Eur. J. Pharm. Sci. 27, 91–99.

Levins, D.M., Glastonbury, J.F., 1972a. Particle–liquid hydrodynamics and mass transfer in a stirred vessel. I. Particle–liquid motion. Trans. Inst. Chem. Eng. 50, 32–41.

Levins, D.M., Glastonbury, J.R., 1972b. Particle–liquid hydrodynamics and mass transfer in a stirred vessel. 2. Mass transfer. Trans. Inst. Chem. Eng. 50, 132–
146.

Lu, A.T.K., Frisella, M.E., Johnson, K.C., 1993. Dissolution modeling: factors affecting the dissolution rates of polydisperse powders. Pharm. Res. 10, 1308–1314.

McCarthy Leonard, G., Bradley, G., Sexton James, C., Corrigan Owen, I., Healy Anne, M., 2004. Computational fluid dynamics modeling of the paddle dissolution apparatus: agitation rate, mixing patterns, and fluid velocities. AAPS Pharm. Sci. Technol. 5, e31.

Misumi, R., Nakamura, N., Nishi, K., Kaminoyama, M., 2004. Effects of instantaneous slip velocity and solute distribution on the dissolution process of crystal particles in a stirred vessel. J. Chem. Eng. Jpn. 37, 1452–1460.

Noyes, A.A., Whitney, W.R., 1897. The rate of solution of solid substances in their own solutions. J. Am. Chem. Soc. 19, 930–934.

Okazaki, A., Mano, T., Sugano, K., 2008. Theoretical dissolution model of polydisperse drug particles in biorelevant media. J. Pharm. Sci. 97, 1843–1852.

Parrott, N., Lave, T., 2002. Prediction of intestinal absorption: comparative assessment of GASTROPLUS and IDEA. Eur. J. Pharm. Sci. 17, 51–61.

Ranz, W.E., Marshall Jr., W.R., 1952. Evaporation from drops. I. Chem. Eng. Prog. 48, 141–146.

Scholz, A., Kostewicz, E., Abrahamsson, B., Dressman, J.B., 2003. Can the USP paddle method be used to represent in-vivo hydrodynamics? J. Pharm. Pharmacol. 55, 443–451.

Sugano, K., Okazaki, A., Sugimoto, S., Tavornvipas, S., Omura, A., Mano, T., 2007. Solubility and dissolution profile assessment in drug discovery. DMPK 22, 225–254.

Wang, J., Flanagan, D.R., 1999. General solution for diffusion-controlled dissolution of spherical particles. 1. Theory. J. Pharm. Sci. 88, 731–738.

Wang, J., Flanagan, D.R., 2002. General solution for diffusion-controlled dissolution of spherical particles. 2. Evaluation of experimental data. J. Pharm. Sci. 91, 534–542.

Wei, H., Loebenberg, R., 2006. Biorelevant dissolution media as a predictive tool for glyburide a class II drug. Eur. J. Pharm. Sci. 29, 45–52.

Yu, L.X., Amidon, G.L., 1999. A compartmental absorption and transit model for estimating oral drug absorption. Int. J. Pharm. 186, 119–125.